

Supplementary Information

The hole in the bucky: structure-property mapping of closed- vs. open-cage fullerene solar-cell blends via temperature/composition phase diagrams

Giovanni Maria Matrone,^a Elizabeth Gutiérrez-Meza,^b Alex H. Balzer,^c Aditi Khirbat,^d Artem Levitsky,^e Alexander B. Sieval,^f Gitti. L. Frey,^e Lee J. Richter,^g Carlos Silva^b and Natalie Stingelin^{*c,d}

DSC heating thermograms taken at a heating rate of 20 °C/min were employed to construct non-equilibrium phase diagrams. For this purpose, we used end-of-melting temperatures of neat components and blends to identify the corresponding solidus lines. When a double endotherm was observed, the one found at lower temperatures was attributed to the eutectic temperatures. For these, the peak temperatures were utilized. Note: data were extracted from the first heating scans which reflect the behavior of the solution-cast films (second heating scans provide information on melt-processed blends). See for more details: Ref S1-3.

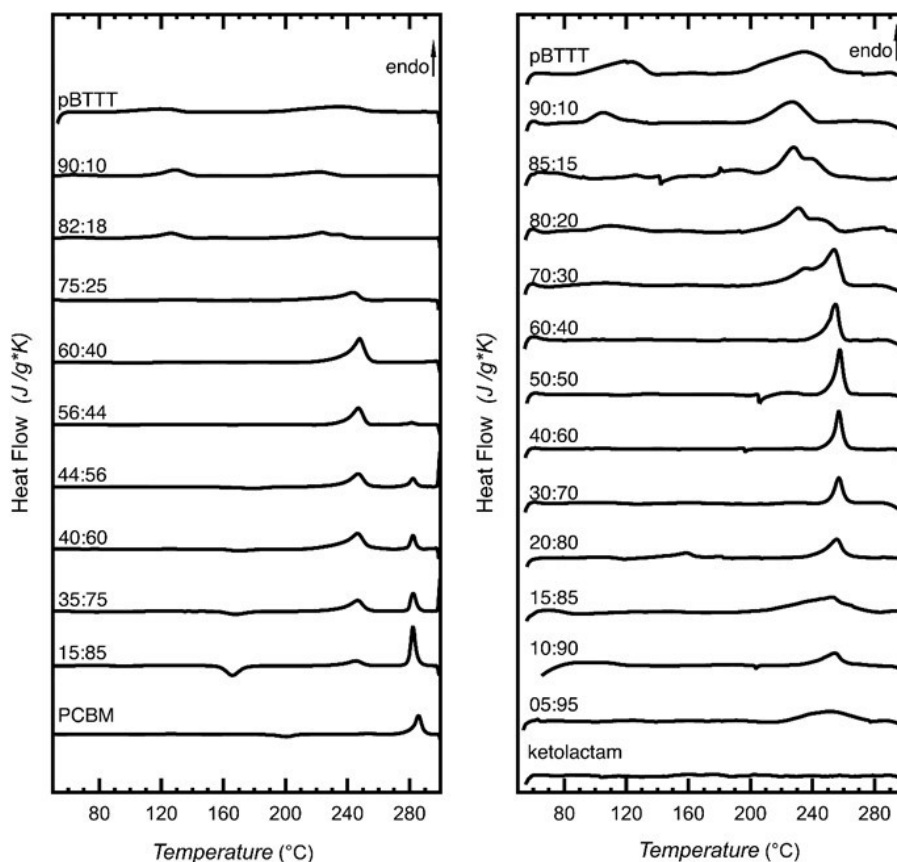


Fig. S1. Differential scanning calorimetry (DSC) first heating thermograms of fullerene:PBTtT blends, recorded at 20 °C/min in N₂-atmosphere on films drop-cast at 40 °C. Note: the thermograms obtained for the PBTtT:ketolactam system were magnified by a factor 5 so that specific features are better discernable.

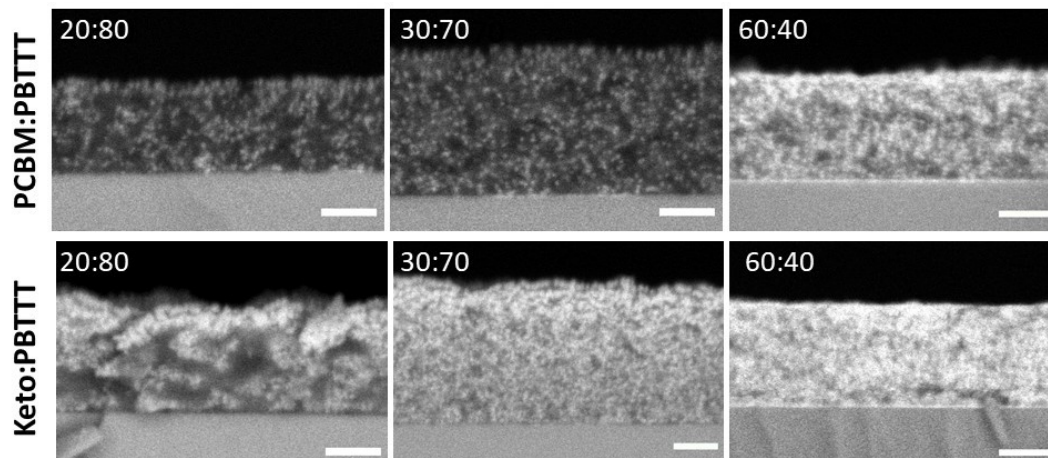


Fig. S2. Cross section BSE HRSEM micrographs of PCBM:PBTTC and ketolactam:PBTTC films after 30 cycles of vapor-phase infiltration (VPI) at 60 °C. The bright contrast in the film represent areas rich in ZnO, indicating PBTTC-rich phase and fullerene:PBTTC intercalated structure, while the dark areas represent the organic phase, indicating the fullerene-rich phase. Scale bar is 100 nm for all the micrographs. More details on the VPI process can be found in Ref. S4.

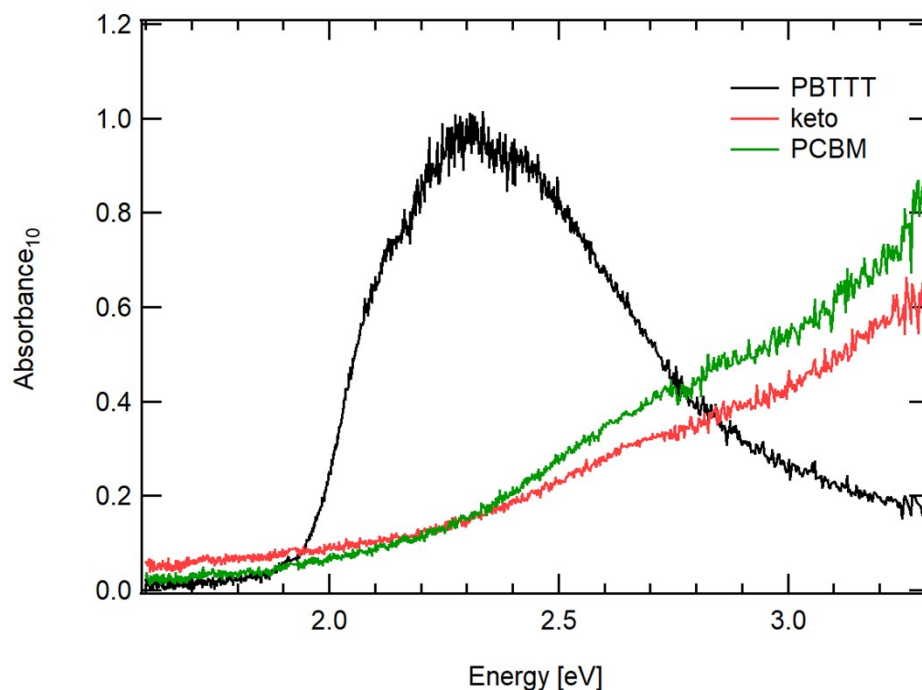


Fig. S3. Linear UV-visible absorption spectra of the two fullerenes used in this work. For comparison the spectra of the neat polymer is shown as well. Note: fullerenes typically coat at a significantly different thickness than the polymer or polymer blends, making a simple comparison problematic. Moreover, the optical density of fullerenes depends on how much they aggregate and their absorption is not strongly structured over the transmission range of, e.g., the glass substrates

In order to gain further insights into the side-chain ordering upon fullerene intercalation, we performed in addition to IR-spectroscopy fast differential scanning calorimetry (FSC) measurements. Fig. S4 depicts the aging/annealing method used to determine the phase transitions of the fullerene:PBTBT blends. This method is analogous to the one used in previous studies.⁵⁻⁷ Samples were initially heated to +400 °C with +4000 °C/s (T_H in Fig. S4) and immediately cooled to the aging/annealing temperature (T_a in Fig. S4) at a rate of -4000 °C /s. At this temperature, samples were aged ($T_a < T_g$) or annealed ($T_a > T_g$) for 30 min and subsequently cooled at -4000 °C to -90 °C (T_L in Fig. S4). The subsequent heating scan at +4000 °C/s to T_H was recorded (heating cycle **a** in Fig. S4). This scan delivered the heat flow rate of aged/annealed samples. Finally, samples were cooled at -4000 °C/s to -90 °C and immediately heated to +400 °C at +4000 °C/s to T_H to obtain the reference thermogram for a sample that was not aged/annealed (heating cycle **b** in Figure S4).

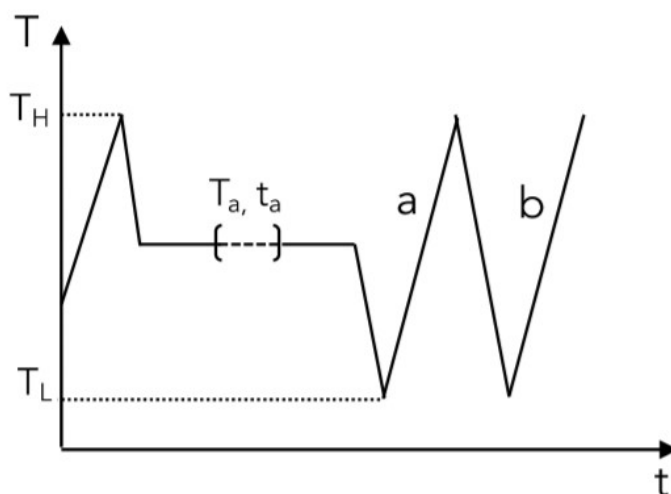


Fig. S4. Temperature program followed for the aging/annealing of polymer samples conducted with Mettler Toledo Flash DSC 1.

We start our discussion with neat PBTBT (Fig. S5). In the reference samples (red curves), we can observe the side-chain softening (around 50 °C) as well as the backbone melting (around 240 °C).⁵⁵ We also observe one enthalpic overshoot (red highlighted area between the heating scan for the annealed sample, black line, and the reference sample, red line) when annealing close or above the side chain softening temperature (around 50 °C), which we attribute to be a result of physical aging.⁵⁶⁻⁸ Moreover, when annealing close or above the liquid-crystalline transition, which in standard differential calorimetry was found to be around 145 °C, other overshoots, in the regime of 100 – 150 °C appear. We use these features (side-chain softening temperature, enthalpic overshoots) to follow the effect of intercalation upon fullerene addition.

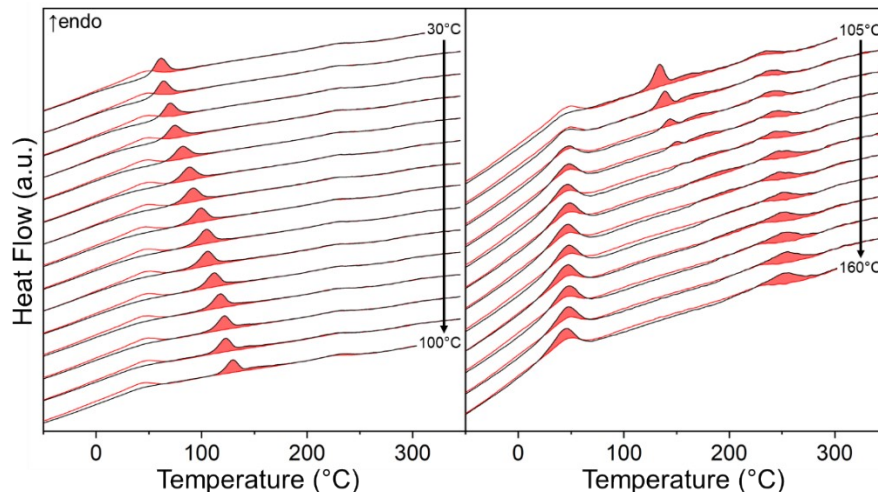


Fig. S5. FSC heating thermograms comparing annealed PBTBT (black) with a reference sample (red). Endothermic overshoots (red highlighted areas) are observed for most annealing temperatures (indicated on the right of the graph, using 5 degree increments). Overshoots in the lower temperature range are attributed to physical aging effects, while the ones between 100 - 150 °C, are attributed to a thermotropic liquid crystalline transition. Higher-temperature annealing leads to increased side-chain organization (≈ 50 °C), deduced from the notably more pronounced endotherm that is recorded.

Addition of the fullerenes into PBTBT leads to a clear decrease in the side-chain softening feature already at a fullerene content of 30 and 50 wt% (Fig. S6), which we assign to an increase in side-chain disorder. This is more pronounced in the PCBM:PBTBT blends where the side-chain melting endotherm cannot be resolved at a fullerene content of ≥ 50 % while for the ketolactam blends ≥ 80 % of the fullerene has to be added to introduce complete side-chain disorder. This can be more clearly seen when comparing the side-chain softening enthalpy to that of the backbone/co-crystal melting in ketolactam:PBTBT blends where we find a clear decrease of the side-chain softening enthalpy compared to the backbone enthalpy (Fig. S7). Note: a similar analysis was not possible to be made with PCBM:PBTBT blends due to the very low enthalpies found for the side-chain softening feature.

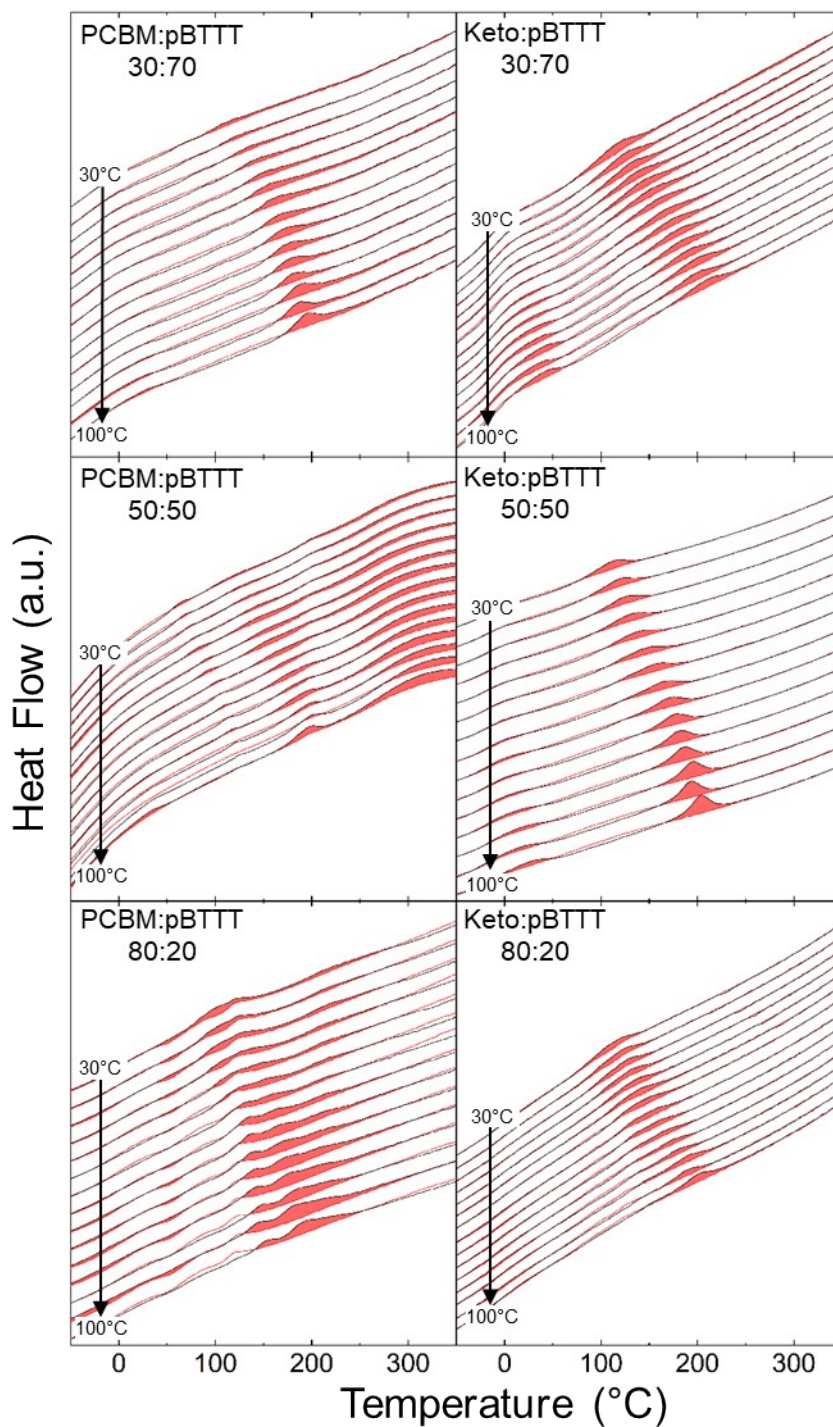


Fig. S6. FSC heating thermograms comparing annealed (black) with unannealed (red) fullerene:pBTTT blends. Endothermic overshoots (red highlighted areas) are observed at most annealing temperatures (indicated on the left of the graph, using 5 degree increments). PCBM:pBTTT blends show a richer phase behavior with a nearly nonexistent side-chain softening feature, indicating the propensity for PCBM to intercalate more than ketolactam leading to high side-chain disorder.

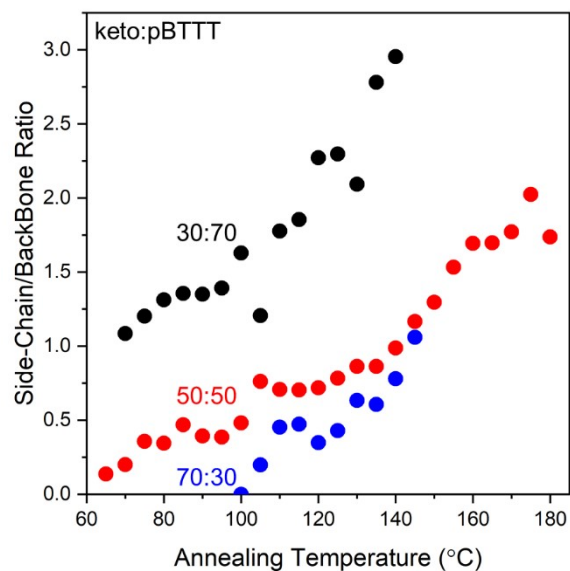


Fig. S7. Ratio of the side-chain softening enthalpy to the enthalpy of the higher temperature endotherm assigned to backbone melting as function of annealing temperature. A larger ratio indicates preferential ordering in the side-chain relative to the backbone/co-crystal.

References:

1. T. Ferenczi, C. Müller, D. D. C. Bradley, P. Smith, N. Stingelin and J. Nelson, *Adv. Mater.*, 2011, **23**, 4093.
2. F. C. Jamieson, E. Buchaca Domingo, T. McCarthy-Ward, M. Heeney, N. Stingelin and J. Durrant, *Chem. Sci.*, 2012, **3**, 485.
3. I. Botiz, M. M. Durbin and N. Stingelin, *Macromolecules*, 2021, **54**, 5304.
4. A. Levitsky, G. M. Matrone, A. Khirbat, I. Bargigia, X. Chu, O. Nahor, T. S. Peretz, A. J. Moule, L. J. Richter, C. Silva, N. Stingelin and G. Frey, *Adv. Sci.*, 2020, **7**, 2000960.
5. D. M. DeLongchamp, R. J. Kline, Y. Jung, E. K. Lin, D. A. Fischer, D. J. Gundlach, S. K. Cotts, A. J. Moad, L. J. Richer, M. F. Toney, M. Heeney and I. McCulloch, *Macromolecules*, 2008, **41**, 5709
6. D. Cangialosi, A. Alegría, and J. Colmenero, in "Fast Scanning Calorimetry", (Eds: C. Schick and V. Mathot), Springer, Switzerland 2016, pp. 403-431
7. J. Martín, N. Stingelin and D. Cangialosi, *J. Phys. Chem. Lett.* 2018, **9**, 990.
8. P. J. W. Sommerville, Y. Li, B. X. Dong, Y. Zhang, J. W. Onorato, W. K. Tatum, A. H. Balzer, N. Stingelin, S. N. Patel, P. F. Nealey, and C. K. Luscombe. *Macromolecules* 2020, **53**, 7511.